Automated 3D Visualization and Documentation for the Analysis of Tomographic Data

C. Rezk-Salama[1], S. Iserhardt-Bauer[2], P. Hastreiter[3], J. Scherer[1],
K. Eberhardt[4], B. Tomandl[4], G. Greiner[1], T. Ertl[2]

[1] Computer Graphics Group, University of Erlangen-Nuremberg, Germany
rezk@informatik.uni-erlangen.de
[2] Visualization and Interactive Systems Group, University of Stuttgart, Germany
[3] Neurocenter, University of Erlangen-Nuremberg, Germany
[4] Division of Neuroradiology, University of Erlangen-Nuremberg, Germany

Abstract. Interactive direct volume rendering has proved to be superior to other methods of 3D visualization since it provides the required quality of 3D representations that is necessary for a detailed diagnosis and planning of surgery. The applicability of direct volume rendering in clinical routine has yet been limited by difficulties in classifying tomographic image data and by the lack of standardized methods to document the visualization results. In this scenario we propose an efficient and reproducible procedure to generate transfer functions for direct volume rendering, which allows to include both medical and technical knowledge. Additionally, we discuss a method to generate digital videos that efficiently document the visualization results. The proposed functionality significantly contributes to the application of direct volume rendering in a clinical environment. As a standardized method it was successfully applied for the analysis of intracranial aneurysms in clinical routine.

Keywords: Visualization, Image Processing, Documentation, Therapy Planning

1 Introduction

Methods of 3D visualization provide the spatial understanding required for a detailed medical diagnosis and planning of surgery. The process of generating visual representations of the information contained in tomographic data is described as a three-tier approach displayed in figure 1. The initial filtering step comprises operations like data conversion, resampling and interpolation. In the subsequent mapping step, abstract data values are transformed into graphical primitives. At this stage visual attributes like color and opacity are assigned. This is often referred to as *classification*, since its major task is to identify anatomical or functional structures based on corresponding data values. The final rendering step uses the graphical primitives and their visual attributes to generate meaningful images.

Fig. 1. The visualization process can be described as a three-tier approach.

For the 3D visualization of medical image data, direct volume rendering based on 3D-texture mapping [1, 2] has proved to be superior to other approaches due to its ability to produce images of high quality at interactive frame rates [3]. Additionally, we have demonstrated its application in medical practice for the analysis of intracranial aneurysms [4] and dural arteriovenous fistulae [5]. However, 3D texture mapping requires high-end graphics hardware which provides the necessary computational power and memory bandwidth. Although there is no doubt about the value of direct volume rendering in clinical routine, its application suffers from some severe limitations.

The first problem concerns the availability of high-end graphics workstations in clinical environments. Above all, it is difficult to justify the high costs of purchase. Furthermore, medical routine needs an adequate and reproducible technique in order to document the results of an examination. According to these requirements, the transfer of large volume data between computers and its loading

into RAM are extremely time-consuming. From our experience this often leads to visualization results which are hardly reproducible and thus they are of minor value for the purpose of documentation.

The problem of hardware availability is partly solved with forthcoming client-server applications [6]. In this scenario the volume data set is uploaded at a remote high-end graphics server via intra- or internet. There, images of high quality are produced by hardware accelerated rendering which are then transferred back to a low-end client application. In the same way, the events of the user interaction are sent to the server which results in modifying the respective viewing parameters. Despite of the technical advantages of this solution, its application is still limited by the classification step because the assignment of transfer functions still requires both the medical knowledge of a physician and the technical know-how of a computer scientist. This problem will be further discussed in section 2 and our solution is presented in section 3.

Due to the interactivity provided by 3D texture mapping the analysis of tomographic data is significantly improved. Above all, motion is extremely important for an optimized spatial understanding, if local illumination is missing. In this context, it is not appropriate to document visualization results by recording static images on the basis of snapshots. In consequence, it is a straight-forward approach to record digital videos. Thereby, visualization is performed efficiently and documentation is performed in a standardized way which permits convenient re-evaluation. In section 4, we introduce an approach for standardized video documentation.

2 Classification

As mentioned above, the analysis of tomographic volumes on the basis of 3D representations requires a classification of the image data which assigns visual attributes to each data value. This assignment is usually performed with transfer functions which map the data values to color and opacity values. In addition to this manual approach, there are several image- and data-driven strategies providing automatic or semi-automatic calculation of the transfer functions.

For correct visual results during volume rendering the position of the transfer function mapping within the rendering pipeline is of major importance. In order to suppress aliasing artifacts the scalar or color values must be interpolated. In this context, the transfer function is either applied prior to the interpolation or subsequently. Correspondingly, there are pre- and post-interpolative transfer functions (see figure 2). Although the pre-interpolative approach significantly avoids artifacts, more precise visual results are only obtained with a post-interpolative transfer function. This is true since continuity is assumed in the data domain, but not in color space. Due to varying capabilities of the underlying graphics hardware, this point is of special importance in order to reproduce direct volume rendering on different platforms.

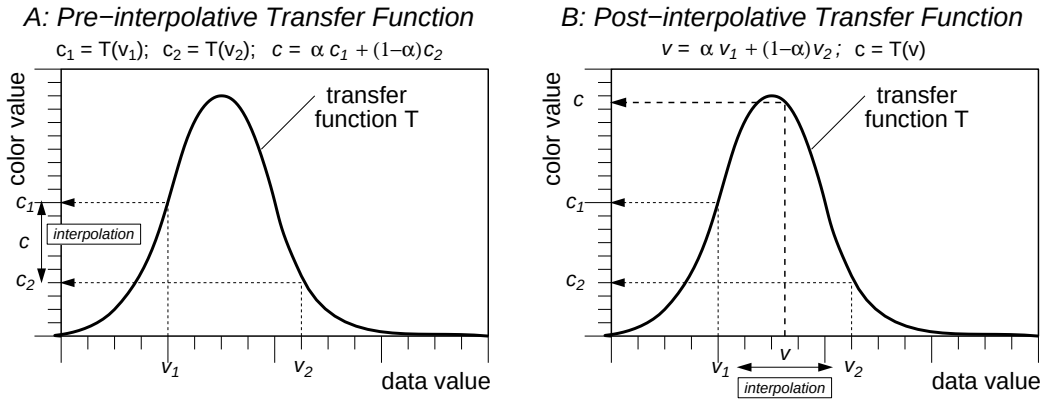

Fig. 2. Applying the transfer function prior to (A) or after the interpolation (B) leads to different visualization results. While pre-interpolative assignment generates smooth images, the post-interpolative strategy produces correct results according to the continuity assumed with the tomographic data model.

In almost every medical application transfer functions for color and opacity are assigned manually using some kind of visual editor. Thereby, implicit segmentation of anatomical structures is performed which is exclusively based on mapping the original data values to display values. The windowing

functionality which defines a linear transformation of the data values is a commonly used 2D example provided with every tool used for medical image processing. In the 3D case more complex transfer functions assign color and opacity.

Since the manual adjustment of transfer functions is usually obtained during an iterative process which is strongly influenced by anatomical knowledge and personal taste of the physician, the whole procedure is rather time-consuming and is difficult to reproduce. A considerable speed-up is achieved with templates defined for a specific modality and pathology [4]. However, this approach strongly depends on the interactivity provided by the rendering procedure since direct visual feedback is indispensable. In contrast to this strategy, different approaches for automatic or semi-automatic assignment of transfer functions have been proposed more recently. They are mainly divided into image-driven and data-driven techniques.

Marks et al. [7] proposed the concept of design galleries in order to set visual parameters in general. This image-driven, semi-automatic method generates a huge amount of images with different parameter settings, allowing the user to select the image with the optimal visual result. Contrary to that He et al. [8] presented an image-driven technique for semi-automatic generation of transfer functions using a stochastic search algorithm. This method generates images using an initial "population" of transfer functions. Having selected the best set of images another stochastic search is started that generates a new population of transfer functions. As a drawback of both image-based approaches, they are neither fast nor easily applicable in clinical routine.

According to data-driven approaches Fang et al. [9] have proposed a technique based on intensity mappings. The transfer function is modeled as a sequence of 3D image processing operations which allows the user to specify qualitative parameters. A related technique was presented by Sato et al. [10]. Their approach applies 3D image filters in order to accentuate local intensity structures using a multi-dimensional feature space. Kindlmann and Durkin [11] suggested an interesting data-driven method. It takes into account the first and second order directional derivative along the gradient direction of the scalar field. However, the original approach is less applicable for the diagnosis of medical image data in practice since anatomical information is not considered. Based on the work of Kindlmann, we introduce a strategy which avoids this drawback. Its main issues are outlined subsequently.

The data values v in direction of the (non-zero) gradient represent a monotonically increasing function $v = f(x)$ as displayed in figure 3. In image processing, the first and second order derivatives $f'(x)$ and $f''(x)$ are frequently used criteria for boundary detection. Since $f(x)$ is monotonically increasing (and thus invertible), it is possible to express the directional derivatives $f'(x)$ and $f''(x)$ as a function of the data value $v = f(x)$ instead of the position x. Therefore, in practice, for each voxel of the original data set the first and second order derivatives in gradient direction are computed. Subsequently these values are averaged for all voxels with a specific data value v. This results in two functions $g(v)$ for the first and $h(v)$ for the second order derivative. Then, the fraction of these two functions is calculated which results in the *position function*

$$p(v) = \frac{-h(v)}{g(v)} \quad . \tag{1}$$

It describes the average distance of a data point with value v from a boundary in the data set assumed by the underlying boundary model. According to Kindlmann, function $p(v)$ is used to compute a transfer function by applying a boundary emphasis function[11]. However, this calculation is not required for our approach.

Although the original algorithm accurately determines boundaries within data sets, its application to different tomographic data is limited, since the specific vislualiztion problem is not taken into account.

3 Automatic Adjustment of Transfer Functions

In order to bridge the gap between automatic assignment and the manual strategy, we present a new approach that combines the advantages of both manual and data-driven techniques. Its basic idea is to use an interactively optimized transfer function as a reference template. This template is manually assigned once for a specific data set. It is then automatically adjusted to other data sets of the same modality by non-linear transformation. In order to search for the optimal distortion of the

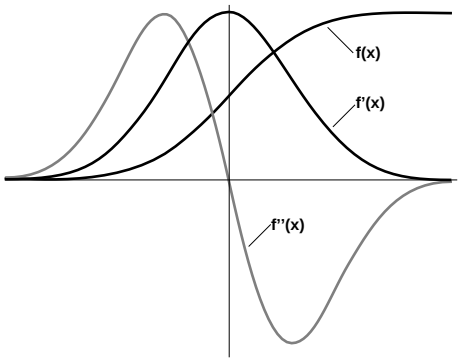

Fig. 3. Function $f(x)$ and first and second order derivatives $f'(x)$ and $f''(x)$ in direction of the voxel gradient.

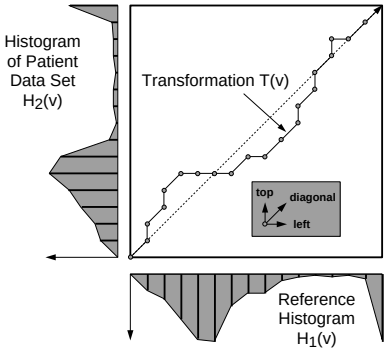

Fig. 4. *Non-linear time warping:* A non-linear transformation $t(v)$ of the data value range is optimized for minimal histogram dispersion using dynamic programming

template function an appropriate similarity metric is required. Based on the concept of *non-linear time warping* [12] the axis of the original data values is distorted non-linearly in order to align the histograms of both data sets. As displayed in figure 4, this is achieved by applying a one-dimensional transformation $t(v)$, which is defined on the range of existing data values v. Suppose there is an optimal transfer function $T_1(v)$ which was found for a specific data set D_1 with a histogram $H_1(v)$. In order to adjust this transfer function to a different data set D_2 of the same modality, dynamic programming [13] is used for optimization. Based on a specific similarity metric the transformation $t(v)$ is computed that optimizes alignment of both histograms to

$$H_2(v) \approx H_1(t(v)) \quad . \tag{2}$$

For normalized histograms a similarity metric D_t is applied that simply measures the distance

$$D_t(H_1, H_2) = \sum_v |H_1(v) - H_2(t(v))| \quad . \tag{3}$$

Note, this metric is monotonically increasing and is thus used as a cost function for the dynamic programming. If the optimal transformation $t(v)$ is found, the same non-linear distortion is applied to adapt the manually assigned transfer function $T_1(v)$ to the new data set D_2, denoted with

$$T_2(v) = T_1(t(v)) \quad . \tag{4}$$

This optimization procedure is an efficient method to use transfer functions which were heuristically established for a specific data set and to adjust them to data sets of other patients. However, using the histogram exclusively turned out to be not accurate enough. In order to improve the results the *position function* $p(v)$ of equation 1 proved to be superior to the histogram.

Figure 5 displays the histogram $H(v)$ and the position function $p(v)$ for different CTA data sets. The significant feature of the histogram is the high peak which is caused by the large amount of soft tissue. However, this characteristic peak has a very limited extent which leads to the reduced accuracy. In comparison to this, the position function $p(v)$ shows more significant features. The transition between the data values of soft tissue and contrast agent is marked by a high peak in $p(v)$ close to the peak in the histogram. To the left of this peak, there is a significant local maximum with (usually) negative value which describes the boundary between soft tissue and fluid. Additionally, the boundary to bone structures is clearly indicated with another local maximum on the right side relative to the peak in the histogram. Since both, the manually assigned transfer function and the position function $p(v)$ strongly depend on specific boundaries in a data set, $p(v)$ represents a more robust basis for the optimization procedure.

4 Standardized Video Documentation

In order to use digital videos for the documentation for 3D visualization results, a standardized recording procedure is required. Usually, clinicians examine individual patient data in a similar way.

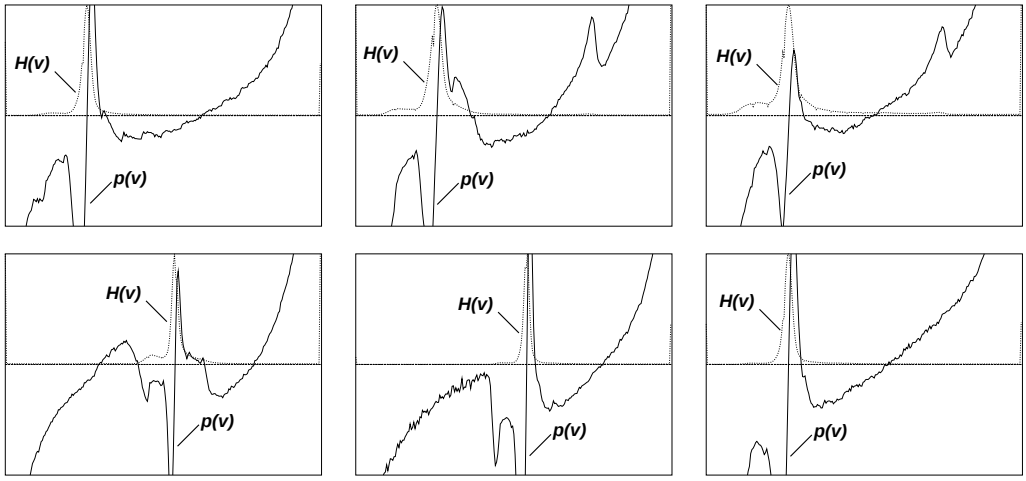

Fig. 5. Comparison of histogram $H(v)$ and position function $p(v)$ for six different CTA data sets of the head

At first, an overview of the complete data set is used for the purpose of orientation and in order to search for pathologic regions. Subsequently, if a suspicious region is found, it is examined in detail from a closer view point. This strategy was taken into account for the presented approach to record digital video in a standardized way.

As a basis a standard protocol must be used for the acquisition of CT or MR image data. This requires to define specific values for orientation, resolution and distance of the tomographic slice images. Additionally, appropriate modality-specific templates must be found in order to adjust transfer functions automatically. Since this is manually performed for only a few typical data sets, anatomical knowledge and personal taste are included at this point. To guarantee complete and adequate documentation of the visualization results, standardized camera paths are defined. They are applied directly within the 3D viewer when recording a video sequence. For each data set of an individual patient, the evaluation process is then described as following:

- **Step 1:** The template of a transfer function is selected according to the modality of the data. It is then automatically adjusted to the individual data set using the technique described in section 3.
- **Step 2:** An animation sequence providing the required overview is recorded as digital video. This is achieved in a standardized way by selecting an appropriate camera path. There are several pre-defined sequences for different clinical applications, e.g. camera path for intracranial vessels in order to search for aneurysms or another camera path tailored for finding vessel malformations within the CSF of the spinal column.
- **Step 3:** Using the overview sequence, the clinician selects interesting or suspicious regions. This is achieved by specifying small subvolumes using axis-aligned clip planes. Subsequently, these subvolumes are extracted from the original data set for a more detailed analysis.
- **Step 4:** A detailed analysis is performed for every subvolume. At this stage different specialized camera paths and transfer function templates are used which are capable of delineating the detail information more clearly.

The standardized camera paths of the presented approach are defined as a sequence of key frames specifying the position and orientation of the camera at different time steps. During animation, NURBS-curves are used to interpolate the position and quaternion interpolation is used for the orientation. Thereby, a smooth motion of the camera is guaranteed. In this context the camera paths for the overview sequence are specifically designed for various applications in clinical routine. Contrary to that the camera paths for the detailed analysis of subvolumes are circular trajectories. They automatically scale with the dimension of the subvolume.

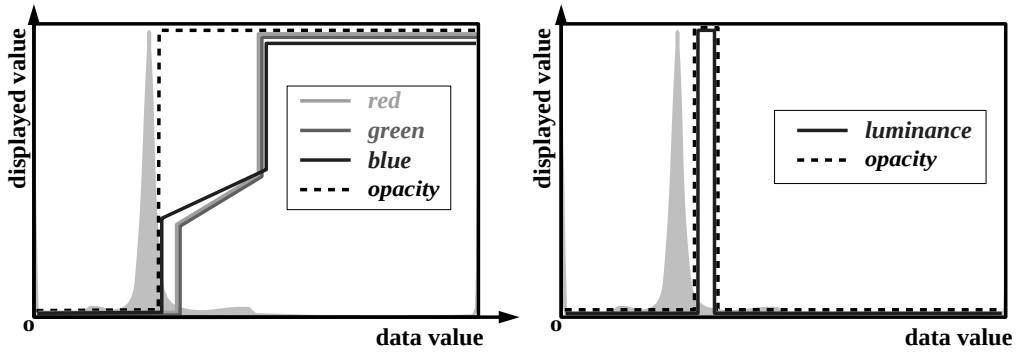

Fig. 6. Different templates of transfer functions are used for an overview (left) and a detailed analysis (right) of intracranial vessel structures.

5 Results and Discussion

The presented functionality was evaluated in a clinical study of 110 patients with intracranial aneurysms. In order to treat these malformations, detailed knowledge of the complex vessel topology and the surrounding critical structures is necessary. Therefore, standard DSA *(Digital Subtraction Angiography)* examinations are supplemented by CT angiography. In this scenario, interactive direct volume rendering of the CTA volume data provides high-quality 3D representations required for surgery planning.

The basis of our study was a scan protocol for CTA with standardized slice distance and field of view. For each patient 64 slice images were acquired using a 512×512 matrix and a resolution of $0.2 \times 0.2 \times 0.5$mm. 100 ml of non-ionic contrast agent was injected with a flow rate of 3 ml/sec and a delay time in dependence of the circulation time.

For the automatic classification of CTA data, templates of transfer functions, as displayed in figure 6 have proved to be useful in clinical practice. The left transfer function is applied for overview images showing the complete vessel information as presented in figure 8A. In this case a completely opaque representation of the vascular structures is envisaged. Additionally, for the anatomical orientation bone structures must be clearly visible. Thus, opacity is set to its maximum for data values that are equal or larger than the value of the contrast dye. The color function is then adjusted in order to differentiate between vessel and bone structures. Since local illumination is not available during rendering, the transfer function for the blue color component was slightly shifted to the left. Thereby, the perception of depth is considerably enhanced by emphasizing vessel boundaries.

In order to provide detailed spatial understanding of the vessel situation in the closer proximity of the aneurysm, a different transfer function template is used (see figure 6, *right*). This leads to a semi-transparent representation, as displayed in figures 8 B.1 and B.2 .

The automatic adjustment was computed using both the histogram based approach and the method based on directional derivatives. For 92 % of the data sets the approach based on the derivatives led to significantly better visual results compared to the histogram based approach (see figure 7). For the remaining 8 % the results of both approaches were almost equivalent.

Volume visualization was performed on an SGI Octane MXE and an SGI Onyx2 with Base Reality Graphics Hardware. For the analysis of intracranial aneurysms a standardized documentation process was developed, as displayed in figure 9. Directly after the adjustment of the transfer function, a clip plane was automatically applied at a fixed position in order to remove the inner cerebral veins located at the back of the head (see figure 9(2)).

Intracranial aneurysms are frequently located at the internal carotid artery, the anterior communicating artery and the bifurcations of the medial cerebral arteries. Therefore, the camera path of the overview sequence starts with an inferior view to the skull base and the carotid and basilar artery. Then, the camera moves on a circular path within the sagittal plane (compare figure 9(3)). Successively, views are provided which show the basilar artery from posterior and finally, the anterior communicating artery from the top. Starting with a lateral position, a second circular camera path is used to fly around the volume data within the axial plane (see figure 9(4)). Since the inner cerebral veins are removed with a clip plane, both paths already provide a comprehensive overview of all

relevant cerebral arteries. For an even more detailed inspection of critical locations the bifurcations of the media cerebral arteries on both sides are additionally approached. This is achieved with a translation of the camera starting with a top view onto the anterior communicating artery.

Throughout our clinical study the presented technique to automatically assign transfer functions has proved to be adequate, robust and reliable. For direct volume rendering the approach based on 3D-textures provides high quality 3D visualization. Additionally, the application of standardized camera paths ensures both comprehensive and reproducible results. Finally, the ability to record digital videos directly within the 3D viewer leads to a fast and efficient documentation applicable in clinical practice. The standardized animation sequences have yet become indispensable for the evaluation and the comparison of results in case of intracranial aneurysms.

6 Conclusion

In order to increase the applicability of direct volume rendering for 3D visualization in clinical environments, we have proposed a reliable method for data-driven classification. Anatomical knowledge is included into the procedure of transfer function assignment by using predefined templates which are automatically adjusted to individual patient data. Furthermore, we propose digital videos as practicable and adequate means of documentation. In this context, the application of standardized camera paths guarantees comprehensive, reproducible and reliable 3D visualization.

The approaches presented in this paper aim at the development of a complex client-server framework for remote 3D visualization. In combination with direct volume rendering which is performed offscreen on a high-end graphics computer, the design of a tele-radiological internet service is envisaged in the future.

References

1. B. Cabral, N. Cam, and J. Foran. Accelerated Volume Rendering and Tomographic Reconstruction Using Texture Mapping Hardware. *ACM Symp. on Vol. Vis.*, pages 91–98, 1994.
2. R. Westermann and T. Ertl. Efficiently Using Graphics Hardware in Volume Rendering Applications. In *Proc. of SIGGRAPH*, Comp. Graph. Conf. Series, 1998.
3. K. Zuiderveld, P. van Ooijen, J. Chin-A-Woeng, P. Buijs, M. Olree, and F. Post. Clinical Evaluation of Interactive Volume Visualization. In *Proc. Visualization*, pages 367–370. IEEE Comp. Soc. Press, 1996.
4. P. Hastreiter, C. Rezk-Salama, B. Tomandl, K. Eberhardt, and T. Ertl. Fast Analysis of Intracranial Aneurysms Based on Interactive Direct Volume Rendering and CT–Angiography. In *Proc. Med. Img. Comput. and Comp.–Assis. Interv. (MICCAI)*. Springer, 1998.
5. C. Rezk-Salama, P. Hastreiter, K. Eberhardt, B. Tomandl, and T. Ertl. Interactive Direct Volume Rendering of Dural Arteriovenous Fistulae in MR-CISS Data. In *Proc. Med. Img. Comput. and Comp.–Assis. Interv. (MICCAI)*. Springer, 1999.
6. K. Engel, O. Sommer, and T. Ertl. A Framework for Interactive Hardware Accelerated Remote 3D-Visualization. In *Proceedings of IEEE TCVG Symposium on Visualization*, 2000.
7. J. Marks, B. Abdalman, P. Beardsley, W. Freeman, S. Gibson, J. Hodgins, T. Kang, B. Mirtich, H. Pfister, W. Ruml, K. Ryall, J. Seims, and S. Shieber. Design galleries: A general approach to setting parameters for computer graphics and animation. In *Proc. SIGGRAPH*, Comp. Graph. Conf. Series, 1997.
8. T. He, L. Hong, A. Kaufman, and H. Pfister. Generation of transfer functions with stochastic search techniques. In *Proc. IEEE Visualization '96*, 1996.
9. S. Fang, T. Biddlecome, and M. Tuceryan. Image-based transfer function design for data exploration in volume visualization. In *Proc. IEEE Visualization '98*, 1998.
10. Y. Sato, C.-F. Westin, A. Bhalerao, S. Nakajima, N. Shiraga, S. Yoshida, and R. Kikinis. Tissue Classification Based on 3D Local Intensity Structures for Volume Rendering. In *Proc. JAMIT Frontier '97*, 1997.
11. G. Kindlmann and J.W. Durlin. Semi-automatic generation of transfer functions for direct volume rendering. In *ACM Symp. on Vol. Vis.*, pages 79–86, 1998.
12. H. Niemann. *Pattern Analysis and Understanding.* Springer Verlag, 2. auflage edition, 1990.
13. S.E. Dreyfuss and A.M. Law. *The Art and Theory of Dynamic Programming.* Academic Press, New York, 1962.

Note to reviewers: the color pages can also be found at
http://www9.informatik.uni-erlangen.de/eng/research/vis/auto/miccai.html

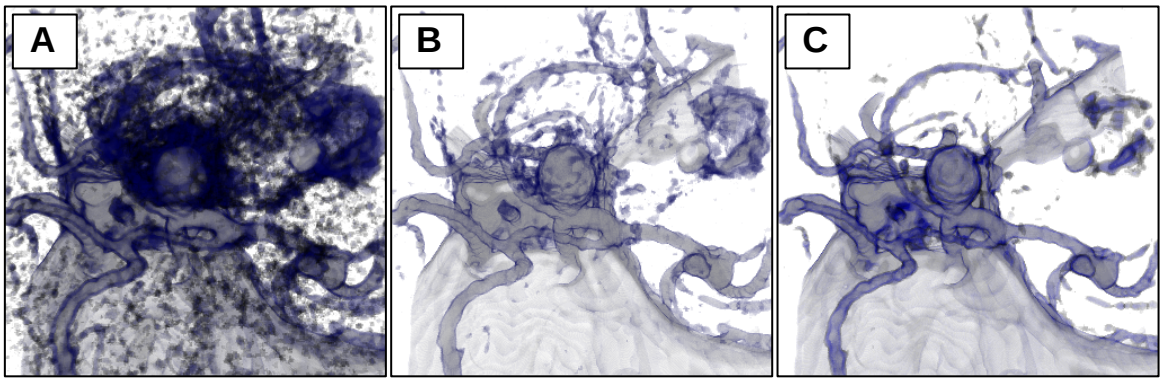

Fig. 7. Applying the transfer function without adjustment (A), with histogram adjustment (B) and with adjustment based on directional derivatives (C)

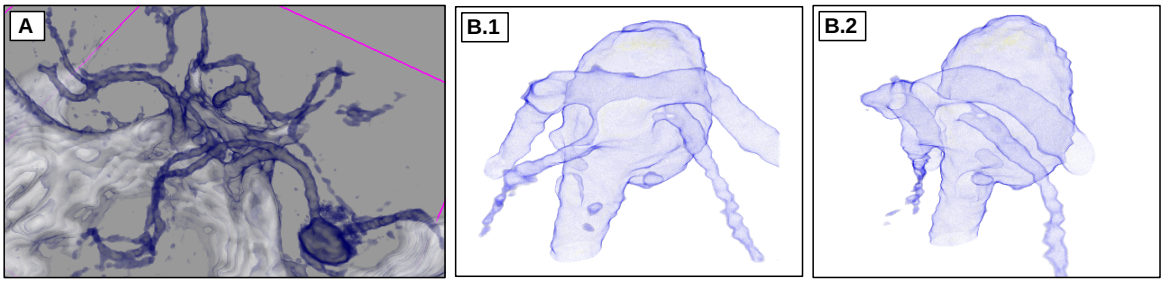

Fig. 8. The transfer function templates presented in Figure 6 have been manually adapted to provide optimal delineation of vascular structures for the overview sequence (A) and for detailed analysis (B)

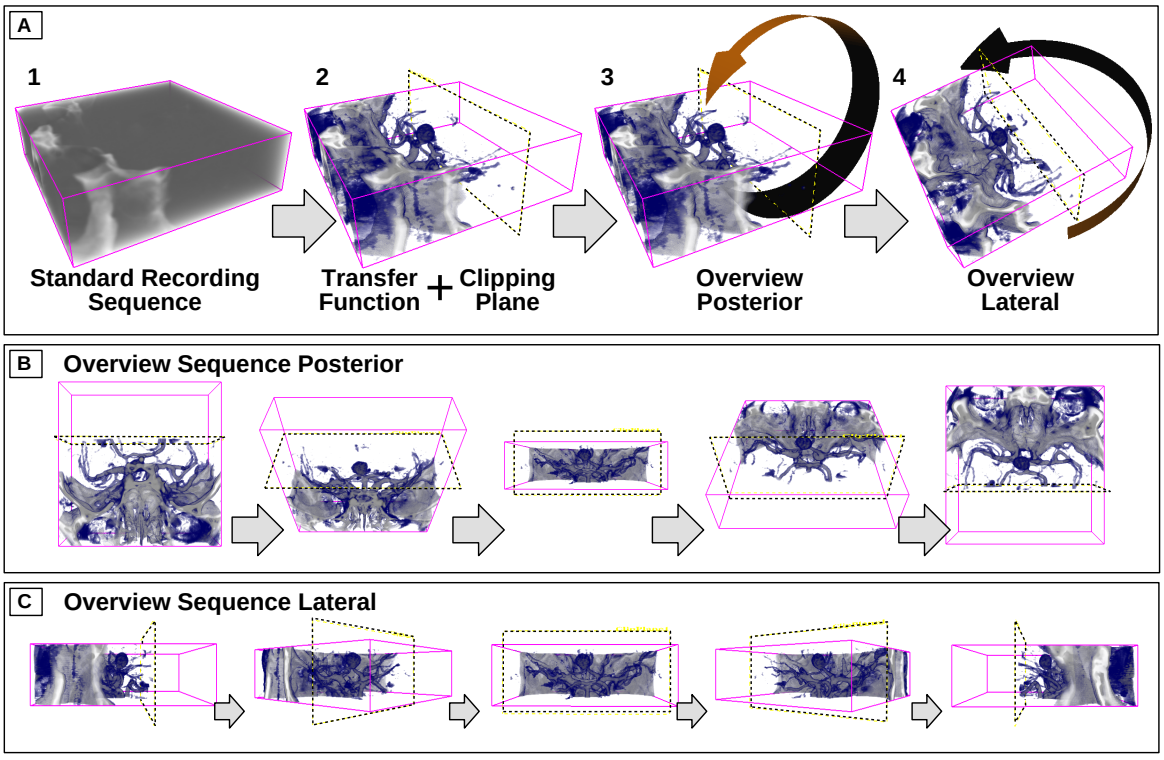

Fig. 9. A standardized procedure (A) has been established for the analysis of intracranial vessels. This procedure comprises camera animation sequences for posterior (B) and lateral (C) overview.